nagra.

Arbeitsbericht NAB 13-37

A model for radionuclide release from spent UO2 and MOX fuel

June 2014

L. Johnson

**Nationale Genossenschaft
für die Lagerung
radioaktiver Abfälle**

Hardstrasse 73
CH-5430 Wettingen
Telefon 056-437 11 11

www.nagra.ch

nagra.

Arbeitsbericht NAB 13-37

A model for radionuclide release from spent UO2 and MOX fuel

June 2014

L. Johnson

KEYWORDS
spent fuel, radionuclide release, fuel dissolution, UO2, MOX, instant release fraction

**Nationale Genossenschaft
für die Lagerung
radioaktiver Abfälle**

Hardstrasse 73
CH-5430 Wettingen
Telefon 056-437 11 11

www.nagra.ch

Nagra Working Reports concern work in progress that may have had limited review. They are intended to provide rapid dissemination of information. The viewpoints presented and conclusions reached are those of the author(s) and do not necessarily represent those of Nagra.

Table of Contents

Table of Contents I

List of Tables II

List of Figures II

1 **Introduction** 1

2 **Characteristics of fuel assemblies at the time of disposal** 3
2.1 Burnup distribution of fuel assemblies 3
2.2 Fission gas release in Swiss reactor fuel 3
2.3 Estimates of the fraction of fission and activation products at grain boundaries (F_{GB}) 6

3 **Evidence for aqueous radionuclide release from fuel assemblies and assessment of data for the radionuclide release model** 9
3.1 Release of radionuclides from Zircaloy and other metal parts of the fuel assemblies 9
3.2 Rapid release of fission products and activation products from spent fuel 9
3.2.1 Correlations of rapid aqueous release (IRF_G) of ^{137}Cs, ^{129}I and ^{36}Cl with FGR 10
3.2.2 Rapid release (IRF_T) of ^{14}C, ^{79}Se, ^{126}Sn, ^{90}Sr, ^{107}Pd and ^{99}Tc 10
3.2.3 Potential release of the inventory at grain boundaries 11
3.3 Fuel matrix dissolution 12

4 **Radionuclide release model and parameter values** 15

5 **References** 17

List of Tables

Table 1: FGR and burnup at the end of the respective cycles (KKB-1/2 6-Region core) (AREVA 2012)..... 4

Table 2: FGR and burnup at the end of the respective cycles for a KKG 5-region-core (AREVA 2010)..... 5

Table 3: FGR of French PWR fuel based on in Fig.1 of Johnson et al. (2005) and fraction of the total fission gas (FG) inventory in a fuel rod that is present in the pores in the rim region of UO_2 fuel with burnup values of 37, 41, 48, 60 and 75 MWd/kgHM. BE – best estimate values; PE – pessimistic estimate values, from Ferry et al. (2009). 8

Table 4: Dissolution rates in ppm yr^{-1} of ^{233}U doped UO_2 in anoxic pore waters containing various concentrations of Cl^- (Ollila 2008) The doping levels of 5% and 10% ^{233}U represent equivalent fuel ages of 10000 and 3000 years respectively. 13

Table 5: Average FGR and IRF (aqueous release) values (%) for radionuclides for spent fuel from the Swiss reactors, including IRF_G (gap), IRF_{GB} (grain boundaries) and IRF_T (total). Red shading represents IRF values that are correlated with FGR (see Section 3.2.1). Blue shading indicates IRF values not correlated with FGR. 15

List of Figures

Fig. 1: Conceptual distribution of radionuclides in a spent fuel rod, based on Johnson and Tait (1997). 1

Fig. 2: FGR at end of cycle (EOC) for UO_2 fuel assemblies at KKB (AREVA 2012)..... 4

Fig. 3: EOC FGR of UO_2 fuel assemblies for KKG 5 region core (AREVA 2010)..... 5

Fig. 4: The FGR at the EOC and for EOL cycles 5 and 6 for Leibstadt (Oldberg 2009). 6

Fig. 5: Photograph of spent fuel showing the high burnup rim region adjacent to the cladding (Fors et al. 2009)..... 7

Fig. 6: Scanning electron microscopy micrograph of the high burnup rim region with a local burnup of 75 MWd/kgHM (Rondinella and Wiss 2010). 7

1 Introduction

The objective of the present report is to provide a model for release of radionuclides from spent fuel for performance assessment calculations as part of SGT Stage 2, including the definition and justification of parameter values for the model.

Discussion of the detailed mechanistic basis of the model is limited, as several recent comprehensive discussions of the relevant processes are available. In the case of processes responsible for rapid release of radionuclides, the discussions in SKB (2010a,b) and Johnson et al. (2012) provide most of the background. For the dissolution rate of the oxide matrix and associated radionuclide release, the detailed reviews of Shoesmith (2008), Curti (2011), SKB (2010a,b) and Ollila (2011) are available.

Figure 1 shows the conceptual distribution in a spent fuel rod of radionuclides relevant to long-term safety assessment. During in-reactor irradiation, a fraction of the inventory of some radionuclides produced in the UO_2 is segregated to grain boundaries, to cracks in the fuel and to the gap between the fuel and cladding. Similarly, a fraction of the fission gas produced also segregates. The majority of the radionuclide inventory resides in the UO_2 matrix and in the cladding.

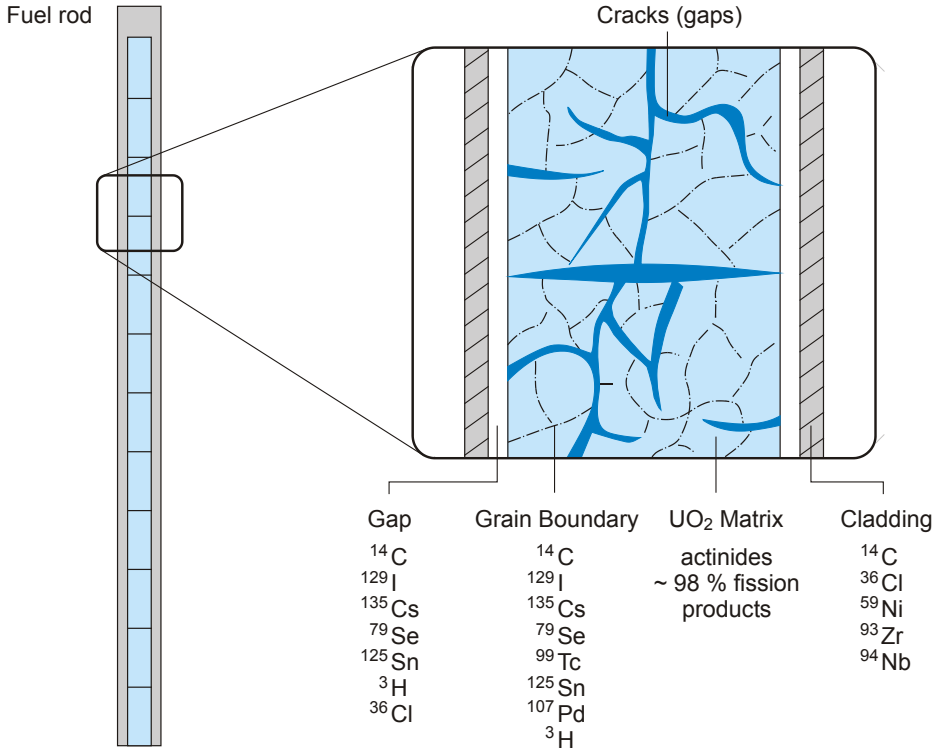

Fig. 1: Conceptual distribution of radionuclides in a spent fuel rod, based on Johnson and Tait (1997).

The distribution of radionuclides within spent fuel rods controls the kinetics of their release into pore water after eventual breaching of disposal canisters. The present report provides both the basis for the distribution of radionuclides and the model for the kinetics of their release from the fuel.

The model for release of radionuclides considers the following processes:

a) Release of activation products from Zircaloy and other metal parts of the fuel assemblies – This involves rapid release of a fraction of the ^{14}C inventory associated with the Zircaloy oxide film, followed by slow release of activation products as a result of corrosion.
b) Release of the so-called IRF (instant release fraction) from the fuel matrix, which is for each radionuclide defined as

$$IRF = IRF_G + IRF_{GB},$$

where IRF_G represents the fraction of the total inventory of the radionuclide in the fuel that is released from the gap (the interconnected void space in the fuel rod) and IRF_{GB} is the fraction of the total inventory of the radionuclide in the fuel that is released from grain boundaries. Release from the gap is analogous to fission gas release (FGR) in that the released radionuclides are present in the gap at the end of fuel irradiation in the reactor. They are assumed to dissolve instantaneously when the Zircaloy cladding is eventually breached by water in the repository. The assumption that IRF_{GB} is also instantaneously released is pessimistic, as discussed in Chapter 3.2.2.

c) Fuel matrix dissolution – The largest fraction of the radionuclide inventory (the remaining fission products and activation products as well as the actinides) is released congruently at the rate the matrix of the fuel dissolves. This is controlled by the geochemical conditions that exist when the canister is breached by ground water.

The various relevant properties of the fuel at the time of disposal are presented in Chapter 2, including the structure, composition and FGR as a function of burnup for the various fuel assemblies.

In Chapter 3, the information base for assessing kinetics of release from spent fuel assemblies is discussed, including corrosion of Zircaloy and structural materials, release of segregated radionuclides and dissolution of the spent fuel matrix.

The model and parameter values for the radionuclide release model are presented in Chapter 4.

2 Characteristics of fuel assemblies at the time of disposal

2.1 Burnup distribution of fuel assemblies

Because FGR is a function of fuel power history, and in general increases with burnup, it is useful to have data on the actual and projected end-of-life (EOL) burnup distributions for fuel assemblies from the various reactors. These distributions are available for fuel assemblies from the Beznau, Gösgen, Leibstadt and Mühleberg reactors. The data have been used in conjunction with the FGR calculations in Chapter 2.2 to estimate average FGR for the various reactors.

2.2 Fission gas release in Swiss reactor fuel

Knowledge of the FGR from spent fuel from the various reactors provides a basis for evaluating the degree of segregation of other elements (Cs isotopes[1], ^{129}I and ^{36}Cl) that are volatile under reactor operating conditions and thus provides a basis for estimating the IRF. FGR in Swiss power reactor fuel is an important operational parameter and is frequently determined in fuel characterization studies. Typically such studies involve examination of fuel assemblies that have been selected because they have operated in the most extreme range of conditions in the reactors, e.g. high burn-up or high linear power rating. Results from such studies are consequently not fully representative of the overall spent fuel assembly population. From the perspective of spent fuel disposal, it is of interest to determine the population distribution and average FGR at reactor discharge end-of-life (EOL) and in some cases end-of-cycle (EOC). Such studies have been performed for Beznau (AREVA 2012), Gösgen (AREVA 2010) and Leibstadt (Oldberg 2009) reactors, based on calculations with FGR codes for all fuel assemblies irradiated in the reactors. These reports also contain comparisons between measured and calculated FGR. The FGR codes used have been approved for fuel rod design calculations by SSM and ENSI (Oldberg 2009). The results are summarized below. Combined with knowledge of the actual burnup of fuel assemblies, this provides a method of estimating the average FGR for fuel assemblies from each reactor.

Beznau

The distribution of FGR for UO_2 fuel assemblies from Beznau is shown in Figure 2. Table 1 shows that the average FGR is about 1.4 to 1.8% for EOC 5, 6 and 7 for average burnups ranging from 54 to 62 MWd/kgHM).

[1] The principal isotope of interest in long-term safety is ^{135}Cs, although the experimental measurements normally are made on ^{137}Cs.

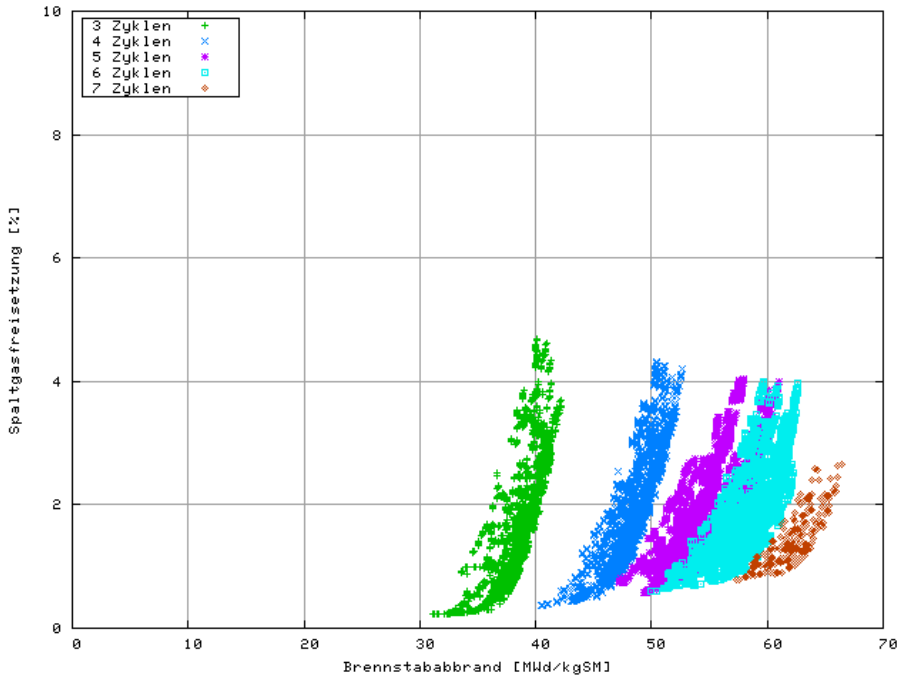

Fig. 2: FGR at end of cycle (EOC) for UO_2 fuel assemblies at KKB (AREVA 2012)

Table 1: FGR and burnup at the end of the respective cycles (KKB-1/2 6-Region core) (AREVA 2012)

	3rd cycle		4th cycle		5th cycle		6th cycle		7th cycle	
	Burnup [MWd/kgHM]	FGR* [%]	Burnup [MWd/kgHM]	FGR* [%]	Burnup [MWd/kgHM]	FGR* [%]	Burnup [MWd/kgHM]	FGR* [%]	Burnup [MWd/kgHM]	FGR* [%]
avg.	37,7	1,4	47,8	1,7	54,3	1,8	57,6	1,8	62,2	1,5
max.	42,1	4,7	52,7	4,3	61,0	4,0	62,6	4,0	66,5	2,7

The average %FGR values at EOC are relatively constant from 40 to 62 MWd/kgHM, indicating that the EOL burnup distribution of fuel assemblies need not be considered; i.e. the significant number of fuel assemblies discharged at burnup values below 50 MWd/kgHM will have similar FGR to those with higher burnup values. As a result an average FGR of 1.8%, characteristic of a burnup of about 58 MWd/kgHM, can be used for all KKB UO_2 fuel assemblies.

For MOX fuel assemblies, the distribution of FGR is shown in Figure 4 of Areva (2012). The average FGR is about 3.4%. Although there are a considerable number of MOX fuel assemblies in storage with burnup values below 35 MWd/kgHM and it is possible they may have low FGR according to Figure 4 in AREVA (2012), this is not further considered here and the average FGR of 3.4% is adopted for KKB MOX fuel assemblies.

Gösgen

The distribution of FGR for UO_2 fuel assemblies from Gösgen is shown in Figure 3 (AREVA 2010). Average EOC FGR values are relatively constant with burnup. For an average EOL burnup of 63 MWd/kgHM, the average FGR is about 13%, as seen in Table 2. This is somewhat higher than for many other pressurized water reactors (PWRs) (Nordström 2009, Johnson et al. 2005). For the purposes of the present report, the average FGR value from the 4th cycle of 14% is adopted for all Gösgen fuel assemblies.

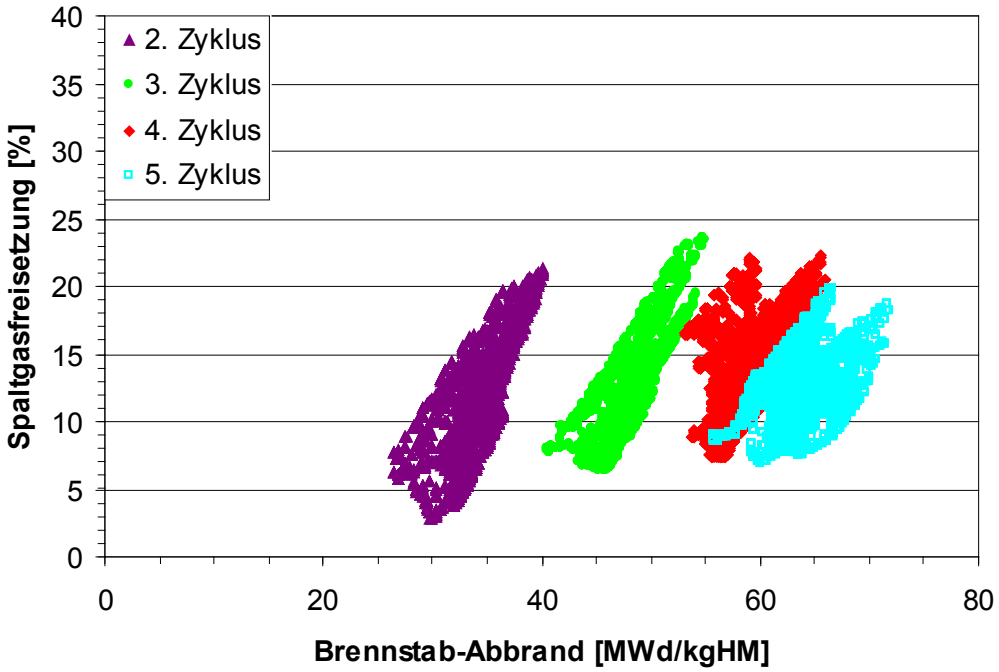

Fig. 3: EOC FGR of UO_2 fuel assemblies for KKG 5 region core (AREVA 2010)

Table 2: FGR and burnup at the end of the respective cycles for a KKG 5-region-core (AREVA 2010)

	2nd cycle		3rd cycle		4th Cycle		5th cycle	
	Burnup [MWd/kgHM]	FGR [%]	Burnup [MWd/kgHM]	FGR [%]	Burnup [MWd/kgHM]	FGR [%]	Burnup [MWd/kgHM]	FGR [%]
avg.	34.7	12.3	48.7	13.0	59.4	14.0	63.5	12.8
max.	40.2	21.2	54.9	23.6	66.0	22.2	71.8	19.9

The distribution of FGR for MOX fuel assemblies from Gösgen is given in AREVA (2010). For an average EOL burnup of 55 GWd/tHM, the average FGR is about 16 %.

Leibstadt

The distribution of FGR for fuel assemblies from Leibstadt is given in Figure 4 (Oldberg 2009). For Cycles 5 and 6, with EOL burnup values in the range of 50 to 65 MWd/kgHM, the average FGR is 4.5 %. That the results in Fig. 4 represent bounding values is indicated by the study of Ledergerber et al. (2010) of lead assemblies from Leibstadt irradiated to rod average burnups of 78 MWd/kgHM, which resulted in all rods having measured FGR below 4.5%. It is noted that for fuel assemblies discharged at burnup values of less than about 40 MWd/kgHM , the average FGR is somewhat lower than 4.5%, possibly about 2.5 to 3%, based on Figure 4. It is thus concluded that an average FGR of 4.5 % represents a pessimistic upper estimate for Leibstadt fuel assemblies.

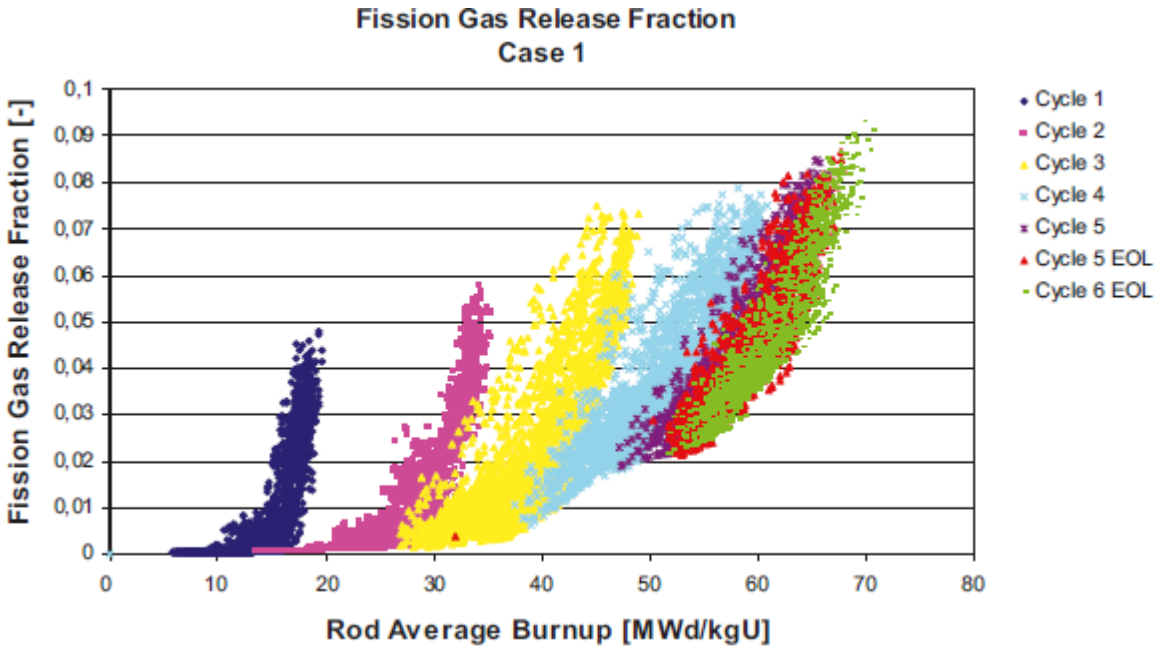

Fig. 4: The FGR at the EOC and for EOL cycles 5 and 6 for Leibstadt (Oldberg 2009).

Mühleberg

The complete distribution of FGR for fuel assemblies from Mühleberg has not been determined. The fuel assemblies are the same as those used in Leibstadt and irradiation conditions are similar, although fuel assemblies at Leibstadt operate at 5-10% higher linear power ratings than at Mühleberg. In the absence of a more detailed analysis, the average FGR for Leibstadt fuel of 4.5% is also assumed for Mühleberg fuel assemblies, which should represent a pessimistic value.

2.3 Estimates of the fraction of fission and activation products at grain boundaries (F_{GB})

Various attempts have been made to estimate the fractional inventory of fission products at grain boundaries using FGR models and evidence from microstructural examination of spent fuel. Accumulation of FG in pores in the rim region (see Figs. 5 and 6) becomes important above an average rod burnup of about 50 MWd/kgHM (Johnson et al. 2005) and the trapped FG can represent a significant fraction of the amount released from the matrix. The most recent

estimates of grain boundary inventories were derived by Ferry et al. (2009) for French PWR fuel and are presented in Table 3, reproduced from Johnson et al. (2012). For typical present-day average burnup values in the range of 55-60 MWd/kgHM, it can be seen that the fraction of fission gas and possibly other volatile radionuclides trapped in pores in the rim is significant. The potential for such material to be released rapidly in water is discussed in Chapter 3.2.

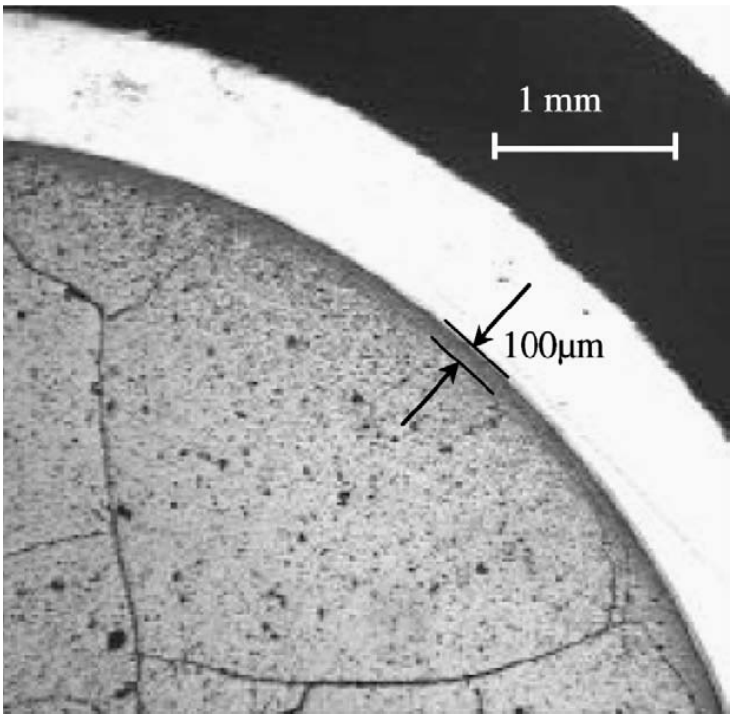

Fig. 5: Photograph of spent fuel showing the high burnup rim region adjacent to the cladding (Fors et al. 2009)

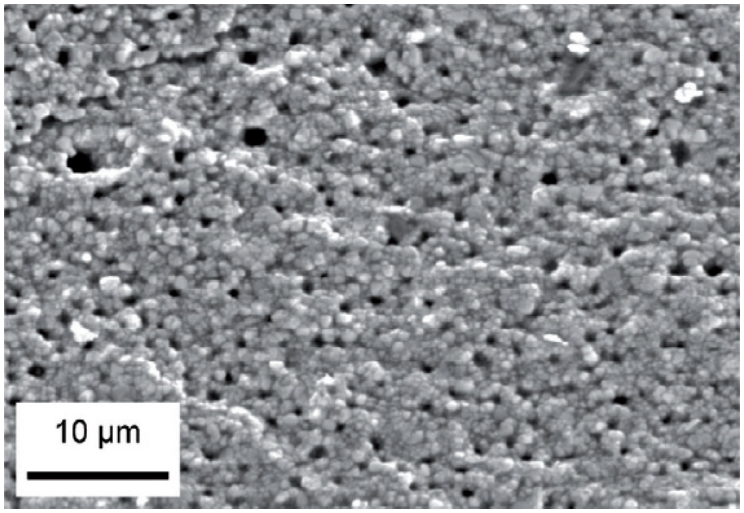

Fig. 6: Scanning electron microscopy micrograph of the high burnup rim region with a local burnup of 75 MWd/kgHM (Rondinella and Wiss 2010).

Table 3: FGR of French PWR fuel based on in Fig.1 of Johnson et al. (2005) and fraction of the total fission gas (FG) inventory in a fuel rod that is present in the pores in the rim region of UO_2 fuel with burnup values of 37, 41, 48, 60 and 75 MWd/kgHM. BE – best estimate values; PE – pessimistic estimate values, from Ferry et al. (2009).

Average burnup (MWd/kgU)	Rim burnup (MWd/kgU)	Typical fission gas release (%)	% of total FG present in the rim pores (BE)	% of total FG present in the rim pores (PE)
37	49	0.3	0	0
41	55	0.4	0	0.5
48	64	1.0	2	3
60	80	3.6	4	8
75	100	~6.5	8	14

In addition to accumulation of fission gas at grain boundaries, some other fission products are also segregated as discussed in Chapter 3.2.

3 Evidence for aqueous radionuclide release from fuel assemblies and assessment of data for the radionuclide release model

3.1 Release of radionuclides from Zircaloy and other metal parts of the fuel assemblies

The corrosion of Zircaloy under repository conditions and the associated radionuclide release were discussed in Johnson and McGinnes (2002), including the results of Yamaguchi et al. (1999) on the rapid release of ^{14}C from the oxide film. No further data on this phenomenon has been reported, thus for performance assessment calculations the assumption of an IRF of 20% is retained. As noted by Yamaguchi et al. (1999), ^{14}C is released in organic form.

No direct measurements of the Zircaloy corrosion rate under repository conditions have been published since the review of Johnson and McGinnes (2002), although a detailed review of the electrochemistry and corrosion behaviour of Zircaloy relevant to a spent fuel repository has been presented by Shoesmith and Zagadulin (2010), who suggested that a corrosion rate of no more than 5 nm yr^{-1} may be expected. A study of the corrosion rate of Zircaloy using a gas evolution method at pH 10.5 in synthetic groundwater containing 0.55 mol/l chloride was reported by Kurashige et al. (1999). The long-term rate decreased to about 1 nm yr^{-1}. A pessimistic value of 10 nm yr^{-1} is selected as a basis for calculating the release rate of radionuclides. For the stainless steel parts of the fuel assemblies, the corrosion rate is also very low. Also based on Kurashige et al. (1999), it is assumed that the corrosion rate-based release of radionuclides from steel parts of the fuel assemblies will occur at a rate of 10 nm yr^{-1}.

The composition, microstructure and corrosion studies of Zircaloy suggest a conceptual model involving some rapid release from the oxide film formed in the reactor, which is typically tens of microns thick, followed by slow corrosion-based release of activation products present in the alloy. The stainless steel parts of the fuel assembly that contain activation products are also expected to be passivated and have low corrosion rates. The specific parameter values for the model are discussed in Chapter 4.

3.2 Rapid release of fission products and activation products from spent fuel

Other fission and activation products besides fission gases are segregated to some degree from the fuel grains as a result of in-reactor irradiation. The behaviour of ^{137}Cs and ^{129}I in spent fuel rods has been widely studied and there is considerable information available on the processes affecting their distribution and release from fuel rods (Johnson et al. 2012). The activation product ^{36}Cl may be even more mobile than ^{137}Cs and ^{129}I (Tait et al. 1997, Pipon 2007). The rapid aqueous release of ^{137}Cs, ^{129}I and ^{36}Cl and the correlations with FGR are discussed in Section 3.2.1. A small fraction of the inventory of ^{14}C is released from the UO_2 grains, although this does not seem to be a thermally driven process, as the aqueous release is independent of fuel power rating (Stroes-Gascoyne et al. 1994). There are many published studies available on the segregation of metallic fission products. In particular, it is well established that there is substantial formation of ε-particles (alloys of Tc, Ru, Mo, Rh and Pd) at grain boundaries in UO_2 fuel. Some other species have been assumed to be segregated from UO_2 to some degree, including ^{79}Se, ^{90}Sr and ^{126}Sn, as discussed in SKB (2010b).

For the various relevant fission and activation products, the sections below discuss the available data on radionuclide segregation and rapid aqueous release. This provides the basis for the instant release fractions (IRF_G and IRF_{GB}) of radionuclides which are then summarized in Chapter 4 for each reactor fuel.

The potential for solid state athermal diffusion of radionuclides in the UO_2 to contribute to the IRF has been examined. As discussed in SKB (2010a), the solid state diffusion coefficient of iodine in UO_2 has been estimated to be less than 10^{-26} m^2 s^{-1}, which would imply negligible diffusive release from UO_2 grains in one million years.

3.2.1 Correlations of rapid aqueous release (IRF_G) of ^{137}Cs, ^{129}I and ^{36}Cl with FGR

The studies reviewed in Johnson et al. (2012) suggest that ^{137}Cs short-term aqueous fractional release is about 1/3 of FGR, although releases are approximately equal in the region of 1 to 2% FGR. On theoretical grounds, assuming diffusion in UO_2 grains is the controlling release mechanism, ^{137}Cs release should be equal to FGR/$\sqrt{3}$ (Lassman et al. 2002), which is selected as bounding as it represents the more pessimistic correlation.

Fractional release of ^{129}I in leaching experiments is often somewhat lower than FGR, but typically does not exceed it (Johnson et al. 2012). Based on diffusion coefficients in fuel under typical irradiation conditions, ^{129}I release should be approximately the same as FGR. Hence, for the selection of the IRF_G value of ^{129}I, a correlation of 1:1 is chosen.

No new data has been published on the aqueous release of ^{36}Cl since the study performed by Tait et al. (1997) on CANDU fuel. In this study, ^{36}Cl release from a number of samples varied from about 10 times FGR at <0.1 % FGR to 3-4 times FGR at 4-8% FGR. CANDU fuel bundles operate at high linear power ratings (high fuel centreline temperature) relative to LWR fuel assemblies (450 W/cm vs. 200 to 250 W/cm). Assuming that the release of ^{36}Cl is thermally driven, the extrapolation of the CANDU data to LWR fuel is uncertain. However, a study of ^{36}Cl diffusion in UO_2 by Pipon et al. (2007) indicated that the high mobility of Cl in spent fuel may arise principally from irradiation-enhanced diffusion. The authors concluded that based on the results, much of the ^{36}Cl produced in LWR fuel could be released to the gap. Because of the various uncertainties, the IRF_G for ^{36}Cl is assumed to be three times the FGR, which represents the best estimate of Tait et al. (1997). A similar ratio is assumed for MOX fuel.

3.2.2 Rapid release (IRF_T) of ^{14}C, ^{79}Se, ^{126}Sn, ^{90}Sr, ^{107}Pd and ^{99}Tc

A number of fission and activation products may be segregated from UO_2 and may be to some extent preferentially released, but without any correlation with FGR. As the releases from grains are uncorrelated with FGR, they are referred to as IRF_T values.

The aqueous release of ^{14}C was measured for CANDU fuel and was found to be independent of fuel power rating (Stroes-Gascoyne et al. 1994), with an average value of 2.7% reported. Johnson and Tait (1997) recommended a bounding IRF_T value of 10% because of the limited number of measurements on LWR fuel, which is adopted here. No new information is available on rapid release of ^{14}C and there is no basis for clearly identifying the chemical form (organic vs. inorganic) of the released ^{14}C.

Attempts have been made to measure the aqueous release of ^{79}Se from LWR fuel. Wilson (1987) was not successful in detecting Se in leaching and from his 'less than' values a maximum release of <0.025% can be derived. Johnson et al. (2012) also attempted to measure ^{79}Se release but were not successful, reporting a 'less than' value of 0.22% derived from the detection limit in the experiments. Given that the fuel samples that they studied had FGR values as high as 27%, it is reasonable to conclude that there is not a significant IRF_G for ^{79}Se. An IRF_T value of 0.2% is therefore proposed for ^{79}Se.

As discussed in SKB (2010), tin is expected to be metallic in fuel (Kleykamp 1985) and non-volatile under fuel in-reactor conditions. The IRF_T values for ^{126}Sn proposed by Johnson and McGinnes (2002) are therefore excessively pessimistic and the IRF_T value of 0.1% is adopted, as proposed in SKB (2010b).

Very limited preferential release of ^{90}Sr is seen in leaching experiments. Johnson and Tait (1997) concluded that the best estimate IRF_T for Sr would be 0.25 %, with 1% as a pessimistic estimate; the latter value is adopted here.

There is significant segregation of some fission product metals in fuel that form alloy inclusions (ε-particles consisting of Tc, Ru, Mo, Rh and Pd). Aqueous releases from such inclusions are extremely small, as noted in Johnson and Tait (1997) and Gray (1999). Prior estimates of large IRF values for Tc and Pd in Johnson and McGinnes (2002) were principally based on the very pessimistic assumptions that the fraction of these fission products in the rim region was up to 16% without consideration for their potential dissolution. These inclusions are essentially noble, thus little if any rapid aqueous radionuclide release is expected to occur from these inclusions (Ramebäck et al. 2000). Consistent with SKB (2010b), it is assumed that the maximum IRF_T for ^{99}Tc and ^{107}Pd is 1%.

3.2.3 Potential release of the inventory at grain boundaries

As discussed in Section 2.3, significant accumulations of FG and potentially other volatile radionuclides can occur at grain boundaries in fuel, in particular in the rim region. In performance assessment calculations in Nagra (2002a), the quantities of fission products that have accumulated in closed pores at grain boundaries have been conservatively considered to be included in the IRF (Johnson and McGinnes 2002). Nonetheless, there is little evidence for such preferential release; on the contrary, the limited studies done suggest that even in aerated water, in which the dissolution rate is much more rapid than under reducing conditions, release from the rim region is difficult to detect (Fors et al. 2009, Johnson et al. 2012, Roudil et al. 2007). These experimental data suggest that the pores in the rim remain closed in contact with water and that the approach of considering the rim region as part of the IRF_T is overly pessimistic. This essentially is the conclusion in the spent fuel dissolution model for SR-Site (SKB 2010a, b), in which only the gap inventory is considered in estimating the IRF_T for the various reactors. The discussion in Section 3.27 of SKB (2010b) clearly illustrates that while there is some conceptual uncertainty in deriving the IRF_T, there is a reasonable basis for arguing that the grain boundary inventories do not contribute to the IRF_T for the burnup range of <50 MWd/kgU). The two principal studies that gave some evidence on this issue are discussed here.

Few long-term experiments have been done under reducing conditions that relate to the possible contribution of slow penetration of grain boundaries by groundwater to the IRF_T. Spahiu et al. (2004) studied release of fission products and actinides from spent fuel with a burnup of 43 MWd/kgHM at room temperature under a hydrogen pressure of 0.5 MPa. Concentrations of fission products such as ^{129}I, ^{137}Cs and ^{90}Sr, whose aqueous chemistry should not be influenced by redox conditions, did not increase over 500 days from the values measured on the first day. Fors et al. (2009) performed experiments with fuel with a burnup of 59 MWd/kgHM, which therefore should have a significant GB inventory according to Table 3, under reducing conditions, where dissolution of the matrix is negligible. The data suggest essentially negligible enhanced Cs or I release, which appears to offer evidence that grain boundaries do not contribute to release under reducing conditions.

In the present study, the assumption is that the best estimate value of the FG in the pores in Table 3 is also applicable to Cs isotopes and ^{129}I (about 4% at 60 MWd/kgU) and that this amount should be defined as the IRF_{GB} and be assumed to contribute to IRF_T, to reflect uncertainties in making long-term extrapolations. This is reflected in the IRF_T summary values presented in Chapter 4.

3.3 Fuel matrix dissolution

Following canister breaching, pore water will come into contact with the spent fuel cladding, which may be rapidly or gradually breached by localized failure (e.g. hydrogen-induced cracking). Radiolysis of water, in particular by alpha particles, will produce both oxidizing and reducing species. The pore water will contain significant quantities of hydrogen from corrosion of steel[2] and of Zircaloy. The hydrogen gas pressure in the near field is expected to be sustained in the region of 6-8 MPa for of the order of 100,000 years (Papafotiou and Senger 2014). Even relatively low concentrations of hydrogen have been shown to have a capacity to maintain a reducing potential on the surface of spent fuel, alpha-doped UO_2 and SIMFUEL[3] (Shoesmith 2008; SKB 2010a,b; Carbol et al. 2009). The experimental studies are supported by detailed modelling studies of radiolytic reactions on a spent fuel surface (Wu et al. 2014), which show that radiolytic oxidation of spent fuel is completely suppressed above a hydrogen concentration of 0.1 µmol/l (H_2 partial pressure of ~10^{-5} MPa). The principal reaction that suppresses oxidative dissolution is the catalysis of the reversible dissociation of H_2 to H• radicals on the noble metal ε-particles present in spent fuel, which protects the galvanically coupled UO_2 matrix from corrosion (Shoesmith 2008). The possibility that such noble metal catalytic surfaces may become poisoned by sulphide present in the repository pore water, thus potentially countering the H_2 effect, was examined by Yang et al. (2013), who concluded that there is no evidence that this occurs. Furthermore, even in the absence of significant hydrogen the oxidative effects due to alpha-radiolysis of water have been shown to be negligible under anoxic conditions and for reducing[4] water containing sulphide or Fe for alpha-doped UO_2 (Ollila 2006, 2008, 2011).

The results lead to two possibilities for a dissolution model for spent fuel. The first is a so-called solubility-limited model. The second is a dissolution rate model, either constant or decreasing with time, based on various lines of evidence, including actual measurements of dissolution rates.

In the solubility-limited model, dissolution of the UO_2 matrix releases U(IV) into solution and aqueous diffusion continuously transports the U(IV) away from the surface into the bentonite backfill. Uranium oxide dissolution is assumed to supply U(IV) at a rate sufficient to maintain the solubility of U(IV) under reducing conditions. This approach was postulated as an alternative model in Chapter 3.2 of Nagra (2002b). The model results in a dissolution rate that decreases from about 5 x10^{-9} yr^{-1} at 10^4 years to 10^{-10} yr^{-1} at 10^6 years. There is no direct experimental evidence of such low dissolution rates, although theoretical considerations and electrochemical data (Shoesmith 2008), as well as the long-term stability of uraninite deposits over geologic time (Cramer et al. 1994), provide some evidence that dissolution rates can indeed be this slow.

The arguments for a dissolution rate model are discussed in some detail in SKB (2010a,b). Based on a number of studies of dissolution of UO_2, alpha-doped UO_2 and spent fuel under anoxic and reducing conditions, they propose a model based on a constant very low dissolution rate. In Sections 3.3.5 to 3.3.10 of SKB (2010b), there is a detailed discussion of the evidence for the expected spent fuel dissolution rate in a repository. The evaluation concludes with an estimate of the fractional dissolution rate with lower limit, best estimate, and upper limit of 10^{-8}, 10^{-7}, and 10^{-6} yr^{-1}. The text states *"The electrochemical model (King and Shoesmith 2004) proposes slightly lower dissolution rates, 10^{-7}–10^{-8} yr^{-1}. Practically the same rates (10^{-6} to 10^{-8} yr^{-1}, with a best estimate at $4 \cdot 10^{-7}$ yr^{-1}) are proposed in Carbol et al. (2005), based on the*

---

[2] It is assumed that carbon steel is used to construct the canister, either as an internal structure that is coated externally with copper, or as the only construction material (Johnson and Zuidema 2013).

[3] SIMFUEL is UO_2 doped with inactive fission products

[4] Anoxic refers to oxygen-free conditions, whereas reducing refers to conditions in which an active reducing agent is present, e.g. H_2, Fe^{2+}, or S^{2-}.

experimental data obtained under the EU-project SFS. In Ollila and Oversby (2005) and Ollila (2006) dissolution rates based on total uranium releases similar to, or lower than, those suggested above are reported for reducing conditions." An illustration of the measured dissolution rates of alpha-doped UO_2 in solutions with various concentrations of Cl^- after up to 91 days is shown in Table 4, taken from Ollila (2008). The ^{233}U doping levels of 5% and 10% represent equivalent fuel ages (i.e. equal alpha-particle dose rates to the solution) of 10000 and 3000 years respectively.

Table 4: Dissolution rates in ppm yr^{-1} of ^{233}U doped UO_2 in anoxic pore waters containing various concentrations of Cl^- (Ollila 2008) The doping levels of 5% and 10% ^{233}U represent equivalent fuel ages of 10000 and 3000 years respectively.

UO_2 sample (1 g)	NaCl I= 0.01 M	NaCl I= 0.5 M	NaCaCl I= 0.625 M	NaCl I= 1 M NaCl
UO_2 – 0% ^{233}U (1)	0.10	0.13	0.08	0.03
UO_2 – 0% ^{233}U (2)	0.20	0.12	0.07	0.05
UO_2 – 5% ^{233}U (1)	0.10	0.11	0.09	0.02
UO_2 – 5% ^{233}U (2)	0.04	0.05	0.04	0.03
UO_2 – 10% ^{233}U (1)	0.04	0.06	0.05	0.02
UO_2 – 10% ^{233}U (2)	0.04	0.06	0.02	0.02

Based on the discussion above, a dissolution rate of 10^{-7} yr^{-1} is proposed for safety assessment calculations. The likelihood that the rate exceeds this value is considered low.

ENSI (2010) has stipulated that Nagra must also perform calculations of radionuclide release from spent fuel in the safety assessment calculations for E2 using both a fuel matrix dissolution rate and a cladding dissolution rate that are one hundred times the reference rates that Nagra proposes for safety assessment.

4 Radionuclide release model and parameter values

Based on the information presented, the basis for modelling radionuclide release from spent fuel can be summarized as follows:

1. Zircaloy corrosion and radionuclide release

IRF_T ^{14}C = 20%

Corrosion rate of Zircaloy = 10 nm yr^{-1}

Assuming a cladding thickness of ~600 μm and corrosion from both sides the radionuclide release rate is:

$$10 \text{ nm yr}^{-1} / 3 \times 10^5 \text{ nm} = 3.3 \times 10^{-5} \text{ yr}^{-1}$$

2. IRF values for spent fuel

The IRF_T is for each radionuclide defined as

$IRF_T = IRF_G + IRF_{GB}$

IRF_G and IRF_{GB} values are defined only for Cs isotopes and ^{129}I. For other radionuclides, only IRF_T values are given. The FGR and IRF values for all reactors for both UO_2 and MOX fuel are presented in Table 5, based on the discussion presented in Chapters 2 and 3. The average IRF_T values in Table 5 for the various fuel types are recommended for the E2 safety assessment calculations.

Table 5: Average FGR and IRF (aqueous release) values (%) for radionuclides for spent fuel from the Swiss reactors, including IRF_G (gap), IRF_{GB} (grain boundaries) and IRF_T (total). Red shading represents IRF values that are correlated with FGR (see Section 3.2.1). Blue shading indicates IRF values not correlated with FGR.

	Beznau		Gösgen		Leibstadt	Mühleberg
	UO_2	MOX	UO_2	MOX	UO_2	UO_2
FGR (avg.)	1.8	3.4	14	16	4.5	4.5
IRF_G - ^{137}Cs, ^{135}Cs	1.8	2.0	7.5	9.2	2.6	2.6
IRF_{GB} - ^{137}Cs, ^{135}Cs	4	4	4	4	4	4
IRF_T - ^{137}Cs, ^{135}Cs	5.8	6	11.5	13.2	6.6	6.6
IRF_G - ^{129}I	1.8	3.4	14	16	4.5	4.5
IRF_{GB} - ^{129}I	4	4	4	4	4	4
IRF_T - ^{129}I	5.8	7.4	18	20	8.5	8.5
IRF_T						
^{36}Cl	5.4	10.2	42	48	13.5	13.5
^{79}Se	0.2	0.2	0.2	0.2	0.2	0.2
^{14}C	10	10	10	10	10	10
^{126}Sn	0.1	0.1	0.1	0.1	0.1	0.1
^{90}Sr	1	1	1	1	1	1
^{107}Pd	1	1	1	1	1	1
^{99}Tc	1	1	1	1	1	1

3. Radionuclide release by dissolution rate of spent fuel matrix

The release of the remaining inventory of radionuclides is assumed to occur as a result of dissolution of the fuel matrix at a rate of 10^{-7} yr^{-1}.

5 References

Areva (2012): Spaltgasfreisetzungsdaten aus dem Kernkraftwerk Beznau, Block 1 und 2 für Studien zur Endlagerung abgebrannter Brennelemente, Nagra Arbeitsbericht, Nagra, Wettingen, Switzerland.

Areva (2010): Spaltgasfreisetzungsdaten aus dem Kernkraftwerk Gösgen für Studien zur Endlagerung abgebrannter Brennelemente, Nagra Arbeitsbericht, Nagra, Wettingen, Switzerland.

Carbol, P., Cobos-Sabate, J., Glatz, J-P., Ronchi, C., Rondinella, V., Wegen, D.H., Wiss, T., Loida, A., Metz, V., Kienzler, B., Spahiu, K., Grambow, B., Quiñones, J. & Martinez Esparza Valiente, A. (edited by K. Spahiu) (2005): The effect of dissolved hydrogen on the dissolution of ^{233}U doped UO_2 (s), high burn-up spent fuel and MOX fuel. Swedish Nuclear Fuel and Waste Management Co, Stockholm, Sweden, SKB Technical Report TR-05-09.

Carbol, P., Fors, P., Gouder, T. & Spahiu, K. (2009): Hydrogen suppresses UO_2 corrosion, Geochim. Cosmochim. Acta73, 4366-4375.

Cramer, J.J. & Smellie, J.A.T. (1994): Final report of the AECL/SKB Cigar Lake analog study. Atomic Energy of Canada Limited Report, AECL-10851, COG-93-147.

Fors, P., Carbol, P., Van Winckel, S. & Spahiu, K. (2009): Corrosion of high burn-up structured UO_2 fuel in presence of dissolved H_2, Journal of Nucl. Mater. 394, 1–8.

Curti, E. (2011): Chemical evolution of spent fuel and Zircaloy under repository conditions, PSI Report TM-44-11-03.

ENSI:2010: Anforderungen an die provisorischen Sicherheitsanalysen und den sicherheitstechnischen Vergleich, ENSI 33/075.

Ferry, C., Piron, J-P., Poulesquen, A. & Poinssot, C. (2009): Radionuclides release from spent fuel under disposal conditions: re-evaluation of the Instant Release Fraction, Mat. Res.Soc.Symp. Proc. 1107, 447–454, Materials Research Society, Warrendale, PA,

Gray, W. J. (1999): Inventories of iodine-129 and cesium-137 in the gaps and grain boundaries of LWR fuels. In: Wronkiewicz D J, Lee J H (eds). Scientific basis for nuclear waste management XXII, Boston, Massachusetts, 30 November – 4 December 1998. Warrendale, PA: Materials Research Society. (Materials Research Society Symposium Proceedings 556), pp 487–494.

King, F. & Shoesmith, D.W.: Electrochemical studies on the effect of H_2 on UO_2 dissolution, SKB TR-04-20, Svensk Kärnbränslehantering AB.

Johnson, L., Ferry, C., Poinssot, C. & Lovera P. (2005): Spent fuel radionuclide source-term model for assessing spent fuel performance in geological disposal. Part I: Assessment of the instant release fraction, J. Nucl. Mater. 346, 56-65.

Johnson, L., Günther-Leopold, I., Kobler Waldis, J., Linder, H.P., Low, J., Cui, D., Ekeroth, E., Spahiu, K. & Evins, L.Z. (2012): Rapid aqueous release of fission products from high burn-up LWR fuel: Experimental results and correlations with fission gas release, J. Nucl. Mater. 420, 55-62.

Johnson, L.H. & Tait, J.C. (1997): Release of segregated nuclides from spent fuel. SKB TR 97-18, Svensk Kärnbränslehantering AB

Johnson, L. H. & McGinnes, D.F. (2002): Partitioning of radionuclides in Swiss power reactor fuels. Nagra NTB 02-07, Nagra, Wettingen, Switzerland.

Johnson, L. & P. Zuidema (2013): Nagra strategy for development of canisters for disposal of spent fuel and high-level waste, Nagra Arbeitsbericht NAB 13-38, Nagra, Wettingen, Switzerland.

King, F. & Shoesmith, D. (2004): Electrochemical studies on the effect of H_2 on UO_2 dissolution, SKB TR-04-20, Svensk Kärnbränslehantering AB.

Kleykamp, H. (1985): The chemical state of the fission products in oxide fuels. Journal of Nuclear Materials, 131, pp 221–246.

Kurashige, T., Fujisawa, R., Inagaki, I. & Senoo, M.: Gas Generation Behaviour of Zircaloy-4 Under Waste Disposal Conditions, 7th International Conference Proceedings on Radioactive Waste Management and Environmental Remediation, ASME, Nagoya, Japan, Sept 26-30, 1999.

Lassman, K.A., Schubert, A., van de Laar, J. & Walker, C.T. (2002): On the diffusion coefficient of cesium in UO_2 fuel, Fission gas behavior of water reactor fuels, Seminar Proc. 26–29, September 2000, NEA, pp. 321-334.

Ledergerber, G., Valizadeh, S., Wright, J., Limbäck, M., Hallstadius, L., Gavillet, D., Abolhassani, S., Nagase, F., Sugiyama, T., Wiesenack, W. & Tverberg, T.(2010): Proceedings of 2010 LWR Fuel Performance/TopFuel/WRFPM, Orlando, Florida, USA, September 26-29, 2010, Paper 0044.

Nagra. (2002a): Project Opalinus Clay - Safety Report , Demonstration of disposal feasibility for spent fuel, vitrified high-level waste and long-lived intermediate-level waste (Entsorgungsnachweis). Nagra NTB 02-05, Nagra, Wettingen, Switzerland.

Nagra (2002b): Project Opalinus Clay: Models, codes and data for safety assessment, Demonstration of disposal feasibility for spent fuel, vitrified high-level waste and long-lived intermediate-level waste (Entsorgungsnachweis). Nagra NTB 02-06, Nagra, Wettingen, Switzerland.

Nordström, E. (2009): Fission gas release data for Ringhals PWRs, SKB Technical Report TR-09-26, Svensk Kärnbränslehantering AB, Stockholm, Sweden.

Oldberg, K. (2009): Distribution of fission gas release in 10 x 10 fuel, SKB Technical Report TR-09-25, Svensk Kärnbränslehantering AB, Stockholm, Sweden.

Ollila, K. & Oversby, V. M. (2005): Dissolution of unirradiated UO_2 and UO_2 doped with ^{233}U under reducing conditions, SKB Technical Report TR-05-07, Svensk Kärnbränslehantering AB, Stockholm, Sweden.

Ollila, K. (2006): Dissolution of unirradiated UO_2 and UO_2 doped with ^{233}U in 0.01 M NaCl under anoxic and reducing conditions, Posiva Report 2006-08, Posiva Oy, Finland.

Ollila, K. (2008): Dissolution of unirradiated UO_2 and UO_2 doped with ^{233}U in low- and high-ionic-strength NaCl under anoxic and reducing conditions, Posiva Working Report 2008-50, Posiva Oy, Finland.

Ollila, K. (2011): Influence of Radiolysis on UO_2 Fuel Matrix Dissolution Under Disposal Conditions: Literature Study, Posiva Working Report 2011-27, Posiva Oy, Finland.

Papafotiou, A. & R. Senger (2014): Sensitivity analysis of gas release from a SF/HLW repository in Opalinus Clay in the candidate siting regions of Northern Switzerland. Nagra Arbeitsbericht NAB 14-010.

Pipon, Y., Toulhoat, N., Moncoffre, N., Bererd, N., Jaffrezic, H., Barthe, M.F., Desgardin, P., Raimbault, L., Scheidegger, A.M. & Carlot, G. (2007): Chlorine diffusion in uranium dioxide: thermal effects versus radiation enhanced effects. In: Dunn D, Poinssot C, Begg B (eds). Scientific basis for nuclear waste management XXX. Warrendale, PA: Materials Research Society. (Materials Research Society Symposium Proceedings 985), NN05-03.

Ramebäck, H., Albinsson, A., Skålberg, M., Eklund, U.B., Kjellberg, L. & Werme, L. (2000): Transport and leaching of technetium and uranium from spent UO_2 fuel in compacted bentonite clay. J. Nucl. Mater., 277, pp 288–294.

Rondinella, V.V. & Wiss, T. (2010): Mat. Today Vol. 13, No. 12, 224-32

Roudil, D., Jegou, C., Broudic, V., Muzeau, B., Peuget, S. & Deschanels, X. (2007): Gap and grain boundary inventories for pressurized water reactor spent fuels, J. Nucl. Mater. 362, 411-415.

Roudil, D., Jegou, C., Broudic, V. & Tribet, M. (2009): Rim instant release radionuclide inventory from French high burnup spent UOX fuel, Mat. Res. Soc. Symp. Proc. Vol. 1193, 627-633 Materials Research Society, Warrendale, PA.

Shoesmith, D. W. (2008): The role of dissolved hydrogen on corrosion/dissolution of spent nuclear fuel, NWMO TR-2008-19.

Shoesmith, D.W. & Zagadulin, D. (2010): The Corrosion of Zirconium Under Deep Geological Repository Conditions, NWMO Report TR-2010-19.

SKB (2010a): Fuel and canister process report for the safety assessment SR-Site, SKB Technical Report TR-10-46, Svensk Kärnbränslehantering AB, Stockholm, Sweden, 2009.

SKB (2010b): Data report for the safety assessment SR-Site, SKB Technical Report TR-10-52 Svensk Kärnbränslehantering AB, Stockholm, Sweden.

Spahiu, K., Cui, D. & Lündström, M. (2004): The fate of radiolytic oxidants during spent fuel leaching in the presence of dissolved near field hydrogen, Radiochim. Acta 92, 625–629.

Stroes-Gascoyne, S., Tait, J.C., Porth, R.J., Mcconnell, J.L. & Lincoln, W.J. (1994): Release of ^{14}C from the gap and and grain-boundary regions of used CANDU fuels to aqueous solutions. Waste Management 14, 385-392.

Tait, J.C., Cornett, R.J.J., Chant, L.A., Jirovec, J., Mcconnell, J. & Wilkin, D.L. (1997): Determination of Cl impurities and ^{36}Cl instant release from used CANDU fuels, Mat. Res. Soc. Symp. Proc. 465, 503-510, Materials Research Society, Pittsburgh, PA.

Wilson, C.N. (1987): Results from Cycles 1 and 2 of NNWSI Series 2 Spent Fuel Dissolution Tests, HEDL-TME 85-22 UC-70, Westinghouse Hanford Company.

Wu, L., Zack Qin & David W. Shoesmith (2014), An improved model for the corrosion of used nuclear fuel inside a failed waste container under permanent disposal conditions, Corr. Sci. 84, 85-95.

Yamaguchi, I., Tanuma, S., Yasutomi, I., Nakayama, T., Tanabe, H., Katsurai, K., Kawamura, W., Maeda, K., Katao, H. & Saigusa, M. (1999): A study on chemical forms and migration behaviour of radionuclides in hull wastes. In: Proceedings of the 7th International Conference on Radioactive Waste Management and Environmental Remediation, ICEM '99, Nagoya, Japan, 26–30 September 1999. New York: American Society of Mechanical Engineers.

Yang, M., Barreiro Fidalgo, A., Sundin, S. & Jonsson, M. (2013): Inhibition of radiation induced dissolution of UO_2 by sulfide – A comparison with the hydrogen effect. J. Nucl. Mater. 434, 38-42.